



# Studies on destruction of silicon tetrachloride using microwave plasma jet

Lifeng Wu, Zhibin Ma<sup>\*</sup>, Aihua He, Jianhua Wang

Province Key Lab of Plasma Chemistry and Advanced Materials, School of Material Science and Engineering, Wuhan Institute of Technology, Wuhan, 430073, China

## ARTICLE INFO

### Article history:

Received 12 January 2009

Received in revised form 17 August 2009

Accepted 19 August 2009

Available online 25 August 2009

### Keywords:

Microwave plasma jet

Atmospheric pressure

Silicon tetrachloride

Nano-silicon

## ABSTRACT

A new method for destroying silicon tetrachloride has been proposed, which is based on a microwave plasma jet that operates at atmospheric pressure using hydrogen as work gas. The influence of input power ( $P$ ) and silicon tetrachloride concentration ( $\varphi$ ) on the percent destruction and removal of  $\text{SiCl}_4$  was investigated. And the reclaimed solid byproducts were characterized by SEM, EDX and XRD. Species in the plasma, which were identified by atomic emission spectroscopy were found to include no halogen. Results indicate that the destruction efficiency of silicon tetrachloride can reach 96% when  $P = 800$  W and  $\varphi = 1.0\%$ , and the main solid byproduct was Si. The silicon deposited on the molybdenum substrate of the plasma reactor was yellow and typical nano-sized particles with grain size of 54 nm.

© 2009 Elsevier B.V. All rights reserved.

## 1. Introduction

The semiconductor industry in the large-scale use of silane produces a large number of halogenated silane in flue gases. Such undesirable waste is usually disposed of by dumping in depots or discharge into the aquatic medium or the atmosphere. This has resulted in increasing contamination of ground water and degradation of tropospheric ozone [1]. Silicon tetrachloride, one of volatile compounds in flue gases, easily brings health hazards in the air. Recently, a number of technologies for destroying such environmental hazards ranging from air pollutants to solid wastes have so far been tested including thermal decomposition [2], catalytic oxidation [3], biofiltration, carbon adsorption, membrane separation, UV oxidation [4], condensation and plasma-based procedures [5–8].

Non-thermal plasmas provide an alternative method for generating highly reactive species, in which electrons are accelerated by the applied electrical field and transfer their energy via elastic and non-elastic collisions with neutral molecules. The reactions occurring under these conditions are usually far from thermodynamic equilibrium and result in destruction associated with higher electron temperatures of 10,000–20,000 K, by contrast, the neutral gas remains at much lower temperatures. This mechanism is useful for the applied energy to generate radicals and excited atomic and molecular species, thereby facilitating the decomposition of contaminant molecules [1]. Although the temperature of a non-thermal plasma is not so highly influential on the destruction

efficiency, an increased temperature facilitates the process. In addition to enhanced destruction and removal, plasma-based chemical processes provide some advantages such as low implementation, operating and capital costs, and modest facility size requirements, in relation to conventional volatile compounds destruction techniques.

The device used in this work for destroying  $\text{SiCl}_4$  is based on the microwave plasma torch (MPT) developed by Moisan et al. in 1995 [9]. The plasma produced provides an effective energy medium for the removal of residues and is highly stable to impedance changes resulting from the introduction of molecular gases, organic compounds or both. In addition, the atmospheric pressure plasma obtained never reaches thermodynamic equilibrium between neutral species, ions and electrons. This produces a plasma jet with high-temperature and high plasma density. For example, typical air plasma jet generated by microwave breakdown has the plasma density of  $\sim 10^{13} \text{ cm}^{-3}$  and a temperature of  $\sim 6000$  K [10]. Therefore, the microwave plasma jet provides a highly unusual and reactive chemical environment in which several plasma-molecular reactions occur. MPJ at atmospheric pressure has gained huge potential from industry in recent years as a clean, high-temperature intense energy source for various applications of material processing [11,12].

## 2. Experimental

Fig. 1a depicts the proposed  $\text{SiCl}_4$  destroying system. The device comprises a magnetron connected to a WR340 rectangular waveguide ( $\text{TE}_{10}$  mode). They are operated at a frequency of 2.45 GHz and their maximal power is approximately 1000 W. The power supply, consisting of a full-wave voltage double circuit, provides the electrical power to the magnetron, which generates the microwave

<sup>\*</sup> Corresponding author.

E-mail addresses: [linwlf28@yahoo.com.cn](mailto:linwlf28@yahoo.com.cn) (L. Wu), [mazb@mail.wit.edu.cn](mailto:mazb@mail.wit.edu.cn) (Z. Ma).

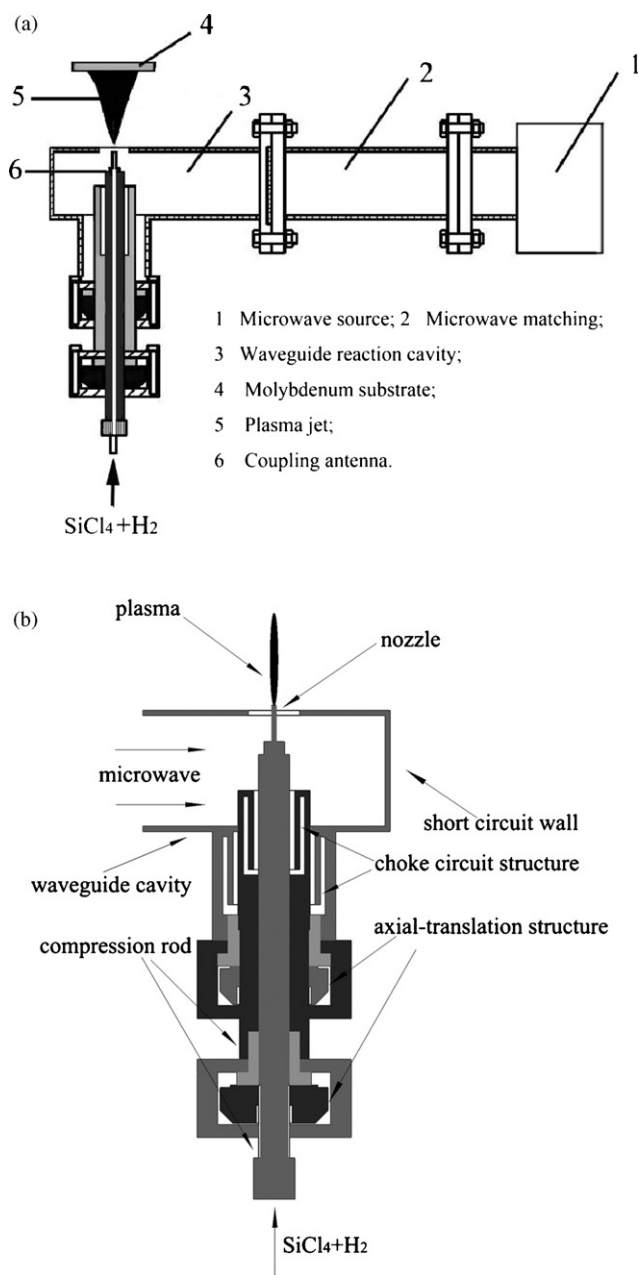


**Fig. 1.** (a) Schematic diagram of the proposed SiCl<sub>4</sub> destruction set-up. (b) Schematic diagram of the plasma reactor.

radiation and is cooled by a water-cooled matched load. The generated microwave radiation from the magnetron is guided through the waveguide, passes through the three-stub tuner, and enters the discharge part [13,14]. The resonant microwave is induced into a copper nozzle located at the centre of the reaction section. The center axis of nozzle is located one-quarter wavelength from the shorted end and is perpendicular to the wide waveguide walls. The electric field induced by the microwave radiation can be maximized by adjusting the three-stub tuner and controlling the following two axial-translation structure to adjust the nozzle position in the cavity. Also, the reflected power adjusted with the three-stub tuner is less than 1% of the forward powder. Choke circuit structure connected with the waveguide can effectively prevent microwave leakage, and a detail of this reactor is shown in Fig. 1b.

For the 2.45 GHz cavity, the modeling results gave the following optimum condition. The nozzle position from the waveguide cavity short circuit wall is 45 mm, nozzle tip diameter is 2 mm, nozzle hole is 0.5 mm, the distance between substrate and nozzle(s) is 20 mm and cavity hole is 20 mm in diameter. This diameter has been optimized to prevent the electrical field from breaking down inside the cavity and also to stop the jet reflected back into the cavity [15]. And the source gases used were hydrogen and liquid compounds (SiCl<sub>4</sub>). Hydrogen was used as a plasma gas and carrier gas with 100 kPa pressure and an 800 ml/min total flow rate. SiCl<sub>4</sub> (99%, Aldrich) in liquid phase maintained at 30 °C was directly bubbled by hydrogen gas and is axially injected through a stainless steel tube, which guides a mixture of bubbled-SiCl<sub>4</sub> and hydrogen (H<sub>2</sub>) gas into the center of the plasma flame. The SiCl<sub>4</sub> concentration (volumetric percentage of SiCl<sub>4</sub> to H<sub>2</sub> flow rates) was varied within a range of 0.8–4%. The flow rates of the silicon tetrachloride and hydrogen were controlled with mass flow controllers. And the solid byproduct was collected by quenching from molybdenum substrate.

In order to observe the surface morphology and structure of the solid byproduct obtained, scanning electron microscopy (SEM) was employed. SEM images of powders as-produced state were recorded on a JSM 5510LV microscope equipped with an EDX analyzer operating at an accelerating voltage of 15 kV. The powder X-ray diffraction (XRD) patterns, obtained with a YB-XD-5A X-ray diffractometer using CuK<sub>α</sub> ( $k = 1.5405981 \text{ \AA}$ ) radiation at a scan rate of  $0.02^\circ 2\theta \text{ s}^{-1}$  were used to determine the identity of any phase present. Spectroscopic analyses of the species present in the plasma during the destruction of SiCl<sub>4</sub> allowed the resulting byproducts to be detected and new pathways for the loss of chlorine and silicon by reaction with copper in the coupler tip to be identified. The monochromator used was WDS-8A which possessed a diffraction grating of 2400 grooves per millimeter.

### 3. Results and discussion

#### 3.1. Destruction of silicon tetrachloride

The SiCl<sub>4</sub> destruction method was optimized by using hydrogen plasma under the most suitable conditions regarding microwave power and SiCl<sub>4</sub> concentration. Hydrogen was primarily considered as a reaction gas, which was injected as the carrier gas of the microwave plasma jet. H<sub>2</sub> is to deoxidize the silicon in SiCl<sub>4</sub>. The powder deposited on the molybdenum substrate was yellow in color. To this end, one should use the percent destruction and removal of SiCl<sub>4</sub>, DRE%, as calculated from the expression:

$$\text{DRE}\% = \frac{W_{\text{in}} - W_{\text{out}}}{W_{\text{in}}} \times 100\%. \quad (1)$$

where  $W_{\text{in}}$  is the mass of SiCl<sub>4</sub> inserted and  $W_{\text{out}}$  that remaining after the plasma treatment.

The principal mechanism for the decomposition of contaminant molecules in a non-thermal plasma is via electron collisions. The efficiency of such collisions increases with increase in the amount of energy released to free electrons in the plasma. Therefore, the efficiency with which contaminants can be destroyed will depend directly on the plasma density and electron temperature, under our experimental conditions:



In fact, the addition of small percentages of a molecular gas can cause a marked variation of the electron energy distribution function in plasmas [16]. Manory et al. [8] have found that the addition of H<sub>2</sub> to a microwave plasma increases the SiCl<sub>4</sub> dissociation. This

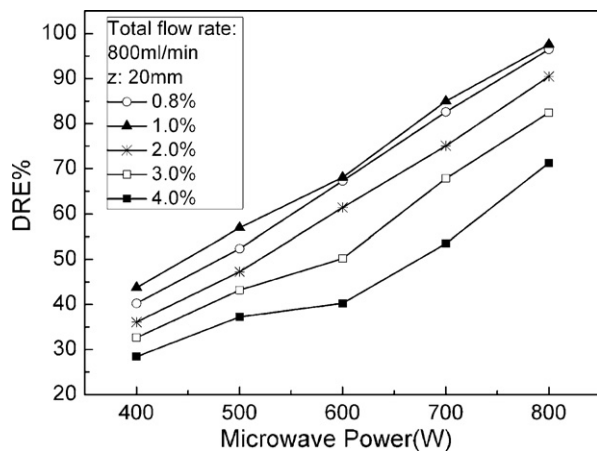


Fig. 2. Variation of DRE% as a function of the supplied microwave power at different SiCl<sub>4</sub> concentration levels.

effect was attributed to the increasing occurrence of the reaction:



The microwave power supplied to the plasma jet via the waveguide has a direct effect as it raises and maintains the electron temperature of the plasma; therefore, increasing the amount of power supplied will result in improved destruction of the compound introduced into the main gas flow.

Fig. 2 shows the variation of DRE% as a function of the supplied microwave power at five different SiCl<sub>4</sub> concentration levels, namely: 0.8%, 1.0%, 2.0%, 3.0% and 4.0%. The total flow rate kept constant at 800 ml/min. As can be seen, at low concentrations, the DRE% increases with increasing concentration introduced in the plasma; above 1.0%, however, the supplied energy is finite and SiCl<sub>4</sub> attains maximum decomposition efficiency at the concentration of 1.0%, and the DRE% decrease with increasing concentration introduced in the plasma correspondingly. At a microwave power settings from 400 to 800 W, the SiCl<sub>4</sub> output concentration decreased and the contaminant destruction efficiency increased with increasing power. A concentration range exists where the destruction efficiency is maximal that changes with the microwave power [17]. The curves are similar in shape for any microwave power, and SiCl<sub>4</sub> concentration above 1.0% leads to an increased output concentrations of SiCl<sub>4</sub> caused by a decreased residence time in the plasma and result in a poorer destruction efficiency. A similar result was previously obtained by Yamamoto and Futamura [18] that can be ascribed to the presence of a secondary destruction pathway involving collisions between chlorine and copper radicals formed in fragmentation reactions preceding the destruction of contaminant molecules. The results are consistent with this assumption but cannot be used to confirm it beyond doubt in the absence of spectroscopic data for the destruction of the plasma itself. Therefore, silicon tetrachloride at these concentration levels can be easily destroyed on an industrial scale by using a moderate microwave power [8].

### 3.2. Characterization of solid byproducts

The SEM images of as-produced Si nanoparticles by the microwave plasma jet are shown in Fig. 3. By comparing samples extracted at different regions, also the difference between the different agglomeration degrees can be found. An agglomerate is equal to just one primary particle at the centre of substrate, whereas it is built up out of many primary particles at the edge. When the plasma has a high degree of particle loading (a high precursor feed rate and higher temperatures), the sample containing particles with

a small degree of agglomeration will show a more open and fluffy structure (Fig. 3a), while the sample containing a high degree of agglomeration shows a dense structure (Fig. 3b). Quenching is the more effective at higher temperatures for centre, and much smaller particles in the agglomerates can be obtained and have a more open structure. EDX survey spectra were used to determine which elements were present in the powder. And silicon specie was detected with mass fraction of 96.3%. The EDX spectra showed an additional line characteristic of the existence of Cl and O. The system was open to the atmosphere in the process of SiCl<sub>4</sub> destruction, as shown in Fig. 1. Therefore, the constituents of the atmosphere may be involved in the destroying process, resulting in possible byproducts during the production of Si nanoparticles. And the as collected powder is of a lower level of oxidation. In addition, the Cu signal is significantly detected due to a little erosion of copper nozzle.

XRD is a powerful tool for determining the structure of as-produced material clearly. Therefore, an XRD pattern of the collected powder was taken, and is shown in Fig. 4. Fig. 4 is the XRD pattern corresponding to SEM images in Fig. 3b. As shown in Fig. 4, black circles indicate the peaks corresponding to Si [space group: *Fd-3m*(227)] with lattice constants  $a = 5.430 \text{ \AA}$ , which are in good agreement with the reported data (JCPDS file No. 65-1060) [19] and white circles correspond to CuCl<sub>2</sub>·H<sub>2</sub>O (JCPDS file No. 33-0451) [20]. And in the process of discharge, detected CuCl<sub>2</sub>·H<sub>2</sub>O in the powder was caused by a little erosion of copper nozzle. In the role of the plasma jet, the high activity copper atoms through high-temperature evaporation move up with the

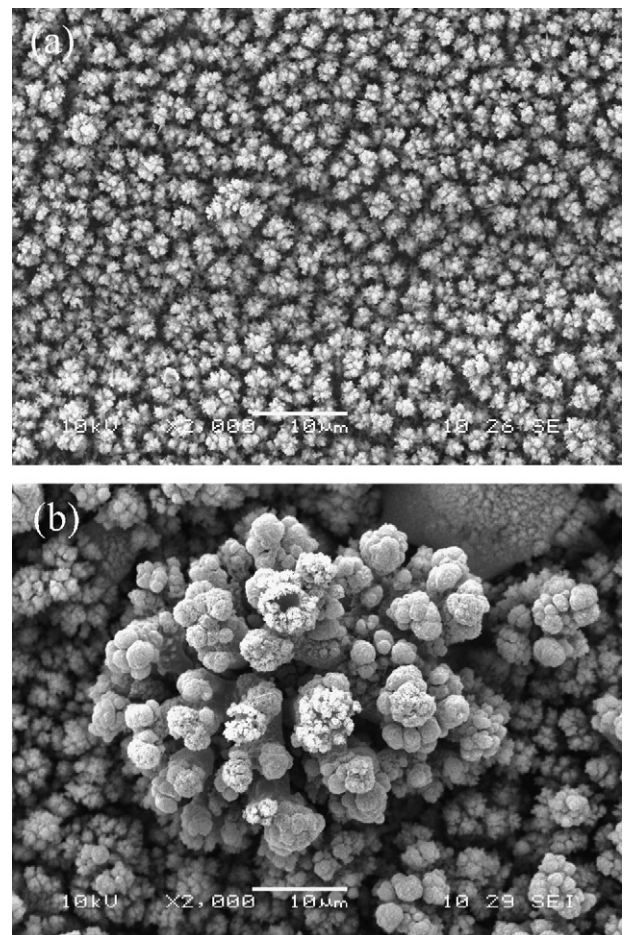


Fig. 3. SEM pictures of Si powders collected at different regions of the molybdenum substrate. (a) Si nanopowder as collected at the centre of substrate and at the edge for (b). Plasma conditions: input power 800 W, 100 kPa, flow rate 800 ml/min.

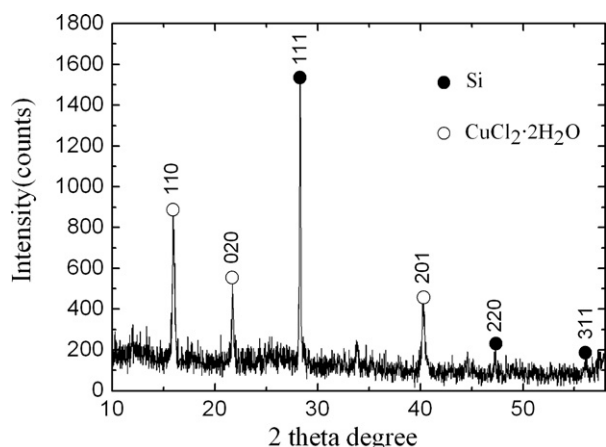


Fig. 4. XRD patterns for the powder deposited on substrate.

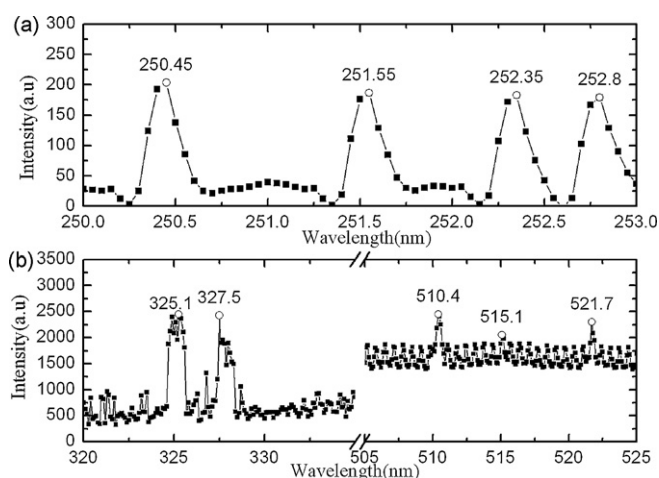


Fig. 5. A part of a typical atomic emission spectrum as measured from a discharge in gases at atmospheric pressure. (a) Atomic emission spectrum of Si during destroying  $\text{SiCl}_4$ . (b) Atomic lines of copper in the process of discharge.

chlorine atoms decomposed from silicon tetrachloride, and precipitate as  $\text{CuCl}_2 \cdot \text{H}_2\text{O}$  crystal when touch the cold-Mo substrate. The Williamson–Hall method [21] can be used to determine the crystallite size and lattice strain when there are three more reflections available for measurement. Contributions of the crystallite size and lattice strain are given by the following equation:

$$\beta \cos \theta = \frac{k\lambda}{L} + \eta \sin \theta \quad (4)$$

where  $\lambda$  is the wavelength of the X-rays ( $\lambda = 1.54 \text{ \AA}$  in this experiment),  $\theta$  is the diffraction angle,  $\eta$  is the lattice strain,  $L$  is the crystallite size,  $k$  is a constant (0.94 for Gaussian line profiles and small cubic crystals of uniform size), and  $\beta$  is the full width at half maximum (FWHM). In Eq. (4), the Si crystallite size was calculated to be approximately 54 nm in the powder.

### 3.3. Spectroscopic analysis of intermediate products

A part of a typical atomic emission spectrum measured from a discharge in gases is given in Fig. 5. The spectrum measurement system can be used to follow relative fluctuations in the gas composition in time. The formation of a little  $\text{CuCl}_2 \cdot \text{H}_2\text{O}$  in the powder from copper in the coupler nozzle was confirmed from its XRD spectrum above, which contained typical lines for copper [Cu I] due to excitation of atoms detached from the coupler nozzle (Fig. 5b). In the case of the MPJ, the carrier gas and  $\text{SiCl}_4$  were mixed before

entering the plasma, and the nozzle material has a strong impact on the plasma properties. The atomic line of copper can be easily distinguished in the shown spectral range between 320 and 525 nm. Several strong atomic lines (325.1 and 510.4 nm) are dominantly present in the measured spectra, as for instance can be seen in Fig. 5b. The number of different atoms which can be observed by emission spectroscopy in the microwave-induced plasmas studied at atmospheric pressure is very limited. In the case of not exceeding the detection limit of grating spectrometer, the wavelength of detection was transferred to a more modest scale. The emission spectra of silicon was detected, as shown in Fig. 5a. Experimentally, it is found that metal such as copper in plasma is more sensitive to changing conditions than silicon. Atomic lines in different wavelength intervals with comparable weak intensities might easily be lost in the analysis process [22]. Therefore, in the process of silicon atomic lines detection, it should try to avoid the interference of copper. To improve the intensity of silicon atomic lines signal, we operate under the optimum condition mentioned above. The range for stable operation in dependence on forward microwave power and  $\text{H}_2$  gas flow was determined experimentally. Stable plasma operation thereby means that the reflected power is less than a few percent of the input power. Moreover, in this region the plasma should exhibit no filaments and a fully symmetrical shape [23].

## 4. Conclusions

The proposed system for destroying volatile contaminants is an effective tool for the removal of silicon tetrachloride. By using the microwave power (800 W) and a flow rate of gas within the optimum range, one can reach an efficiency decomposition level. Based on the analysis of byproducts, the  $\text{SiCl}_4$  is mainly transformed into nano-silicon with grain size of 54 nm under optimum conditions and such nano-materials have very great prospects for industrial application.

In addition, the main pathway for the loss of chlorine is the formation of a copper chloride deposit on the molybdenum substrate. This is consistent with the spectroscopic measurements and XRD, based on the intensity of the atomic line of Cu and diffraction peaks of  $\text{CuCl}_2 \cdot \text{H}_2\text{O}$ . And  $\text{CuCl}_2 \cdot \text{H}_2\text{O}$  is less toxic and easier to handle than  $\text{SiCl}_4$ . Also, it can be used for various purposes. Therefore, the proposed method suppresses the most serious hazards of the initial compound by fixing chloride in a solid, non-volatile form.

## References

- [1] S.J. Rubio, M.C. Quintero, A. Rodero, J.M. Fernandez Rodriguez, Assessment of a new carbon tetrachloride destruction system based on a microwave plasma torch operating at atmospheric pressure, *J. Hazard. Mater.* 148 (2007) 419–427.
- [2] E.C. Moretti, N. Mukhopadhyay, VOC control—current practices and future-trends, *Chem. Eng. Prog.* 89 (1993) 7.
- [3] J.J. Spivey, Complete catalytic-oxidation of volatile organics, *Ind. Eng. Chem. Res.* 26 (1987) 2165–2180.
- [4] M. Mohseni, Gas phase trichloroethylene (TCE) photo oxidation and byproduct formation: photolysis vs. titania/silica based photocatalysis, *Chemosphere* 59 (2005) 335–342.
- [5] T. Oda, T. Takahashi, K. Tada, Decomposition of dilute trichloroethylene by nonthermal plasma, *IEEE Trans. Ind. Appl.* 35 (1999) 373–379.
- [6] G. Bruno, P. Capezzuto, G. Cicala, F. Cramarossa, Mechanism of silicon film deposition in the RF plasma reduction of silicon tetrachloride, *Plasma Chem. Plasma Process.* 6 (1986) 109–125.
- [7] A.V. Gusev, R.A. Kornev, A.Yu. Sukhanov, Preparation of trichlorosilane by plasma hydrogenation of silicon tetrachloride, *Inorg. Mater.* 42 (2006) 1023–1026.
- [8] R. Manory, A. Grill, U. Carmi, R. Avni, Decomposition and polymerization of silicon tetrachloride in a microwave plasma. A mass-spectrometry investigation, *Plasma Chem. Plasma Process.* 3 (1983) 235–248.
- [9] M. Moisan, R. Grenier, Z. Zakrzewski, The electromagnetic performance of a surfatron-based coaxial microwave plasma torch, *Spectrochim. Acta Part B.* 35 (1995) 584–592.
- [10] Dong Hun Shin, Chan Uk Bang, Yong Cheol Hong, Preparation of vanadium pentoxide powders by microwave plasma-torch at atmospheric pressure, *Mater. Chem. Phys.* 99 (2006) 269–275.

- [11] I. Ahmed, Al-Shamma'a, Stephen R. Wylie, Jim Lucas, Jiu Dun Yan, Atmospheric microwave plasma jet for material processing, *IEEE Trans. Plasma Sci.* 30 (2002) 1863–1871.
- [12] H.S. Uhm, Y.C. Hong, D.H. Shin, A microwave plasma torch and its applications, *Plasma Sources Sci. Technol.* 15 (2006) 26–34.
- [13] Yong C. Hong, Hyoung S. Kim, Han S. Uhm, Reduction of perfluorocompound emissions by microwave plasma-torch, *Thin Solid Films* 435 (2003) 329–334.
- [14] J. Hubert, M. Moisan, A. Richard, A new microwave plasma at atmospheric pressure, *Spectrochim. Acta, Part B* 33 (1978) 1–10.
- [15] A.I. Al-Shamma'a, S.R. Wylie, J. Lucas, C.F. Pau, Design and construction of a 2.45 GHz waveguide-based microwave plasma jet at atmospheric pressure for material processing, *J. Phys. D: Appl. Phys.* 34 (2001) 2734–2741.
- [16] G. Bruno, P. Capezzuto, Mechanism of silicon film deposition in the rf plasma reduction of silicon tetrachloride, *Plasma Chem. Plasma Process.* 6 (1986) 109–125.
- [17] S.J. Rubio, A. Rodero, M.C. Quintero, Application of a microwave helium plasma torch operating at atmospheric pressure to destroy trichloroethylene, *Plasma Chem. Plasma Process.* 28 (2008) 415–428.
- [18] T. Yamamoto, S. Futamura, Nonthermal plasma processing for controlling volatile organic compounds, *Combust. Sci. Technol.* 133 (1998) 117–133.
- [19] A. Kohno, N. Aomine, Y. Soejima, A. Akasaki, Anomalous behaviour of silicon single-crystals observed by X-ray diffraction, *Jpn. J. Appl. Phys. Part 1* 33 (1994) 5073.
- [20] Natl. Bur. Stand, Monogr, Plane-wave scattering-matrix theory of antennas and antenna-antenna interactions, *J. Chem. Phys.* (1981) 18–33.
- [21] G.K. Williamson, W.H. Hall, X-ray line broadening from filed aluminium and wolfram L'elargissement des raies de rayons x obtenues des limailles d'aluminium et de tungsteneDie verbreiterung der roentgen interferenzlinien von aluminium- und wolframspaenen, *Acta Metal.* 1 (1953) 22.
- [22] E.A.H. Timmermans, F.P.J. de Groote, J. Jonkers, A. Gamero, A. Sola, J.J.A.M. van der Mullen, Atomic emission spectroscopy for the on-line monitoring of incineration processes, *Spectrochim. Acta Part B.* 58 (2003) 823–836.
- [23] H.W. Herrmann, I. Henins, J. Park, G.s. Selwyn, Decontamination of chemical and biological warfare (CBW) agents using an atmospheric pressure plasma jet (APPJ), *Phys. Plasmas* 6 (1999) 2284–2289.